To the Graduate Council:

We are submitting herewith a thesis written by J. Todd Coleman entitled "Laser-Based Optical Fiber Absorbance Probes for Clinical Analyses." We have examined the final copy of this thesis for form and content and recommend that it be accepted in partial fulfillment of the requirements for the degree of Master of Science, with a major in Chemistry.

Michael Sepaniak

Michael J. Sepaniak, Major Professor

Jerome F. Eastham

Jerome F. Eastham, Major Professor

I have read this thesis
and recommend its acceptance:

Ehrenberg

Accepted for the Council:

Lawrence Dinkel

The Graduate School

LASER-BASED OPTICAL FIBER ABSORBANCE PROBES FOR CLINICAL ANALYSES

A Thesis

Presented for the

Master of Science

Degree

The University of Tennessee, Knoxville

J. Todd Coleman

June 1984

ACKNOWLEDGEMENTS

The author would like to acknowledge several friends and acquaintances:

Dr. Michael J. Sepaniak and Dr. Jerome F. Eastham for their unselfish contribution of guidance, knowledge, and time;

The University of Tennessee, Knoxville, Department of Chemistry, for my graduate teaching assistantship;

Donald S. Acuff, M. D., Baylor University Medical Center, and Pennell Painter, Ph. D., The University of Tennessee Memorial Hospital and Research Center, for their help in procuring cerebral spinal fluids;

Ed. B., Chuck K., Tony B., Mike C., Bruce T., David W., Paul F., and Robert Y. for their many interruptions, mind relaxing sessions, and thought provoking discussions;

My parents, Jerry L. and Dean R. Coleman, for their love, understanding, and financial help for over a quarter of a century;

My fiancé, Susan Elaine Acuff, for her motivation when I had none, for her patience when I was impatient, for her understanding when I could not, and most of all her devotion to me, her fiancé.

ABSTRACT

Conventional bio-analytical techniques generally involve in-vitro measurements of chemicals in extracted samples of fluids or tissues. Unfortunately, a close correlation between a chemical's concentration in an extracted sample and its concentration in the living system is not guaranteed. Remote spectroscopic measurements are now preformed routinely. However, bulky equipment and large sample volumes generally prohibit in-vivo analysis using current technology.

Design variations of a previously developed fluoroprobe make it possible to preform in-vivo chemical absorption measurements. I have developed an absorption probe consisting of a single optical fiber encased in a blunt hypodermic needle with a highly reflective surface affixed at the end of the needle, thus forming a micro-absorbance cell. The blunt needle is inserted inside a larger needle to form a cannula. By aspirating through the inner needle, biological fluid is drawn into the microabsorbance cell. The sample is irradiated with monochromatic light and, using a beam splitter, the non-absorbed radiation is measured with a photomultiplier tube. Corrections are made for scattered radiation also.

There are numerous potential clinical applications for the absorption probe. Our attention was focused on the monitoring of bilirubin, a degradation product of the hemolysis of erythrocytes, in body fluids using the absorption probe. Quantitation of bilirubin in cerebral spinal fluid and amnionic fluid would be helpful in the

diagnosis of a cerebral vascular hemorrhage and erythroblastosis fetalis, respectively. This thesis contains descriptions of the construction of the experimental prototype, optimization experiments, and in-vitro experiments to exemplify the in-vivo capabilities. Comparative analysis was conducted to confirm the values obtained by the absorption probe method. Linearity, limits of detection, and linear dynamic range are also reported.

TABLE OF CONTENTS

LIST OF FIGURES

CHAPTER I

INTRODUCTION

The clinical laboratory has depended on spectroscopy, almost from the start, as a method of analysis for many different compounds in the diagnosis and treatment of illnesses. The different types of spectroscopy include visible absorption, ultraviolet absorption, flame emission, fluorometry, and nephelometry (1). With large volumes of analyses burdening the clinical analyst, a need quickly developed for a method whereby an analyst could perform many analytical tests in a reasonable amount of time with accuracy and precision. Recognizing this need, the first automated system was made commercially available in 1957 by Technicon Instruments Corporation, Tarrytown, New York (1). The original automated system has had many modifications since its first production. Now, those instruments designed to process many samples simultaneously are referred to as sequential multiple analyzers (SMA). The SMA can typically analyze twelve samples simultaneously at the rate of sixty per hour. Sequential multiple analyzers typically work on the continuous flow principle using a peristaltic pump. Automatic analyzers utilize colorimeters, flame photometers, fluorometers, and ultraviolet/visible absorption spectrophotometers for detection (1). For

---

NOTE: Patent is pending through the University of Tennessee Research Corporation on the in-vivo absorbance probe apparatus and other considerations described herein.

spectrophotometric measurements a bichromatic method is usually employed to correct for interfering species (2). The following compounds and elements are routinely assayed in the clinical laboratory using a sequential multiple analyzer bichromatic method: albumin, alcohol, calcium, total bilirubin, cholesterol, chloride, glucose, lactic acid, magnesium, and phosphorus (2).

Automated analyses have increased the efficiency of the clinical laboratory. Nevertheless, there are still several time consuming steps that are common to most all analyses. These steps are outlined below.

1. Patient is scheduled for appointment with physician and/or support personnel.

2. Patient may be moved to a special laboratory or procedure room for removal of sample.

3. Removal of sample by physician and/or support personnel.

4. Sample pick-up and delivery to the clinical laboratory.

5. Protein separation by precipitation, filtration, centrifugation, chromatography, or dialysis.

6. Addition of one or more reagents and incubation.

7. Detection.

8. Signal processing.

9. Data presentation to physician.

Another area that has seen rapid maturity in recent years, like automated analysis, is the science of fiber optics. Technological advances have made it possible to manufacture flexible fiber

optics. Patents proposing image-carrying fiber optic bundles were filed in 1926 (3). The first true working model of a fiber optic bundle was developed in 1930 by Lamm (4). Around 1950 it was discovered that by cladding the optical fiber with a coating of lower refractive index than the fiber core, internal reflections were enhanced, thus increasing the transmitting efficiency. By 1958 research groups had begun experimenting with optical fibers.

Improvements of the first fiber optic system have allowed the use of fiber optics in clinical medicine. Fiber optics have expanded the world of endoscopy since its first trial in 1877 using a hollow tube, a candle, and a sword swallower (5). The first gastroscopes were made of a series of lenses, sometimes as many as fifty, which did not provide the needed flexibility. Therefore, the gastroscope could not conform to the internal shape of organs, subsequently causing "blind spots." Bundles of fibers have led to the production of many different types of endoscopes designed to allow viewing of internal organs in a relatively unobtrusive manner. Many endoscopes are commonly used today (e.g., bronchoscopes, thoracoscopes, cardioscopes, urethascopes, etc.) (2).

Fiber optic bundles have applications other than just simply viewing organs. Fibers have been used in oxymetry, plethysmography (6), and cardiac catheterization (7). In these applications radiation of a specific wavelength is transmitted through a fiber optic bundle into a region of interest. Diffusely reflected radiation is transmitted from this region, via a separate bundle of fibers, to a

photomultiplier tube outside the body for processing of the signal. Given predetermined correlations between oxygen saturation (8), circulatory activity (9), or cardiac output (9,10), and reflected radiation, quantitative clinical information may be obtained. Other medical uses for fiber optic bundles include transillumination, surgical illumination (in particularly confining regions), ophthalmoscopic instrumentation (6), probes for internal examination of solid tissues, photo-induced cancer chemotherapy, and in therapeutic applications such as placement of miniaturized dosimetry tubes used to detect small radiation doses deep in tissues (6).

Some nonmedical uses of fiber optics include communications, remote analysis of uranium, and remote pH measurements (12). Hirschfeld has successfully immobilized chromophoric reagents on fiber termini for subsequent reaction in remote fiber fluorescence (RFF) (13,14). Other researchers have immobilized pH sensitive reagents on polyacrylamide spheres, contained in permeable capsules which encased the fiber terminus, for remote pH monitoring (15).

Current fiber optic bundle technology has led to the development of instrumentation for remote spectroscopic measurements (15). Thus, it is now possible to place the spectrophotometer, or at least the sample cell, in the sample rather than vice versa. Remote spectroscopic measurements have advantages that cannot be realized with conventional removal of a sample for analysis. Among these possible advantages are no disruption of equilibrium, no removal and, therefore, no subsequent disposal of sample, no reduction in the volume of

analyte, reduction in analysis time, safer obtrusion into hostile environments, continuous monitoring, and no exposure to ambient light.

There is, however, a need to improve on current remote absorbance measuring technology, if it is to be used in the clinical analysis field. Currently, the instrumentation used for remote absorbance measurements is too bulky to be used to be considered for in-vivo measurements (16). The equipment that is being used for in-vivo measurements produces relative data (15), that is, no true analytical values, such as absorbances.

I have developed a single quartz fiber probe that is suitable for in-vivo analysis that can measure true absorbance values. The sample cell is contained inside a hypodermic needle which makes it suitable for subcutaneous insertion and autoclaving. The advantages of a laser make it a superior light source for the absorbance probe over a conventional incandescent source. These advantages include large spectral power density and small divergence of colliminated beams (17). In addition to the advantages mentioned earlier that are inherent to remote spectroscopic measurements, the in-vivo absorbance probe possesses other advantages. Due to the construction design, the probe requires an extremely small volume of fluid to fill the sample cell (nanoliters). After the analysis the fluid may be removed or expelled from the probe back into the patient. The absorbance probe is also inexpensive to construct. With the wide use of lasers in the hospital today, existing laser equipment can be adapted for use with the absorbance probe, thus reducing the initial expense in equipment and set-up.

The instrumentation should have a significant impact on the clinical laboratory. Several of the very time consuming and costly steps previously mentioned that are inherent in present clinical analyses can be reduced or eliminated completely. For instance, in a hospital where a central laser can be connected to each patient's room via a flexible fiber optic, bedside analyses may be performed. Immediately, there is no need to remove the patient to a special laboratory or procedure room, no pick-up and delivery of sample to the clinical laboratory (because there is no sample), and no special instructions for handling of sample. Since detection and signal processing are done simultaneously, with the insertion of the probe by a physician, data presentation from the laser technician to the physician can be done without delay by intercom. In some cases, this will reduce the time required in the hospital and subsequently the cost to the hospital and patient. Operation of a health institute under diagnosis related group (DRG) exemplifies the need for cost reducing technology (18).

A typical situation where the absorbance probe could be used is the detection and quantitation of bilirubin (Figure 1), a degradation product in the hemolysis of red blood cells. Quantitation of bilirubin in cerebral spinal fluid and amnionic fluid is helpful in the diagnosis of a cerebral vascular accident or erythroblastosis fetalis. Specifically for bilirubin analyses, the in-vivo absorbance probe method possesses distinct advantages over conventional clinical methods. For instance, the "sample" is never exposed

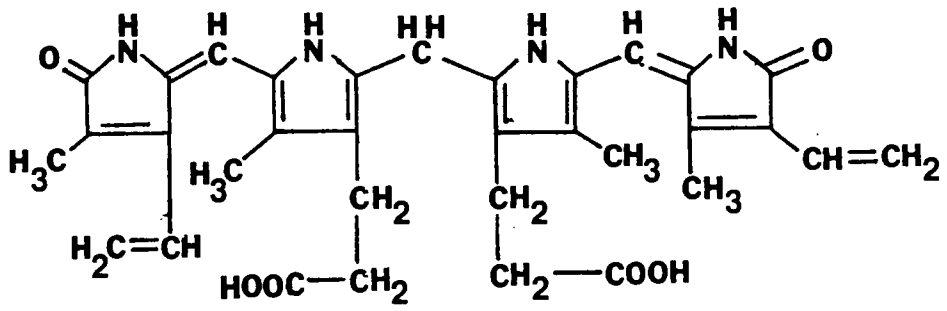

Figure 1. Bilirubin structure.

to ambient light. This removes any possibility of photodegradation of bilirubin prior to analysis, thus giving erroneously low results. The probe can also be used for continuous monitoring. The probe could sustain its in-vivo status indefinitely to monitor dynamic conditions.

For analyses where addition of reagents to the fluid is required prior to spectroscopic analysis, the reagents may be immobilized at the fiber terminus for subsequent reaction after insertion of the absorbance probe, as mentioned earlier. The absorbance probe can also be adapted for bichromatic analyses. Since many clinical analyses utilize bichromatic methods, as stated earlier, this is an important feature of the probe. Bichromatic analyses may be accomplished using the instrumental design shown and described in the Appendix.

In this work in-vitro analyses of cerebral spinal fluids and human serum for bilirubin will be discussed to exemplify the in-vivo capabilities of the absorbance probe. Also, probe design considerations, probe optimization experiments, and relevant interpretation of analytical data will be discussed.

CHAPTER II

EXPERIMENTAL

The apparatus used in this work consists of two parts, the absorbance probe and the instrumentation. The following is a description of how the absorbance probe was constructed and the instrumentation assembled.

The absorbance probe is constructed (Figure 2) by inserting a 600 μm quartz optical fiber into a 19 gauge x 1-1/2" hypodermic needle that has been prepared in the following way. The hypodermic needles were specially made by Becton-Dickinson, New Jersey, to have a smoother more reflective inner wall than conventional disposable hypodermic needles. The hypodermic needles were prepared by drawing stainless steel tubing through dies, first with and then without, an internal mandrel, in decreasing gauges to the final gauge size. The tubing is then straightened out and fabricated into needles. This type of needle visibility provided a greater transmittance of the laser radiation than conventional needles.

The hypodermic needle was then drilled with four 0.015" diameter holes approximately 1-1/4" from the hub of the needle. Next, the hypodermic needle is cut approximately 0.045" from the four previously drilled holes leaving a 90° bevel. The needle is now thoroughly cleaned and any remaining metal burs produced by the drilling process are carefully removed so as not to scar the inner wall of the hypodermic needle. A piece of aluminum foil (2 mm x

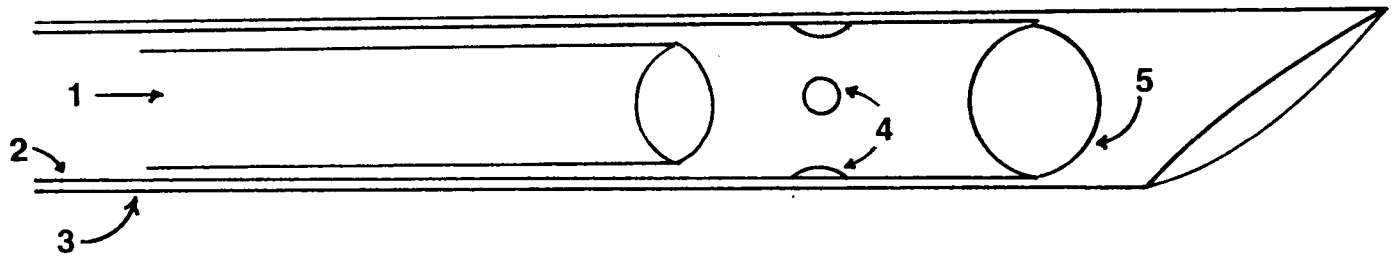

Figure 2. Internal absorbance probe design. (1) Fiber core, (2) 19 gauge hypodermic needle, (3) 15 gauge hypodermic needle, (4) aspiration holes, (5) aluminum reflector.

2 mm x 0.02 mm) is attached at the 90° bevel with optically transparent epoxy. This attachment is done under 30X magnification. Care must be taken to ensure that the 0.045" holes are not clogged with epoxy, so the hypodermic needle is attached to a tuberculin syringe and then placed in a holder positioned under a microscope. After room temperature drying (about 12 hours) the needle is inserted into a 15 gauge x 2" hypodermic needle that does not possess a hub to form a cannula. The 15 gauge needle may be silver soldered to the 19 gauge needle to firmly attach the two needles together. The syringe barrel to which the cannula is attached has been previously adapted for aspiration. Biological fluid is drawn into the sample irradiation cavity, inside the 19 gauge needle between the fiber terminus and aluminum foil, by aspiration. Reduction in the diameter of the fiber optic will allow a hypodermic needle with a smaller diameter to be used, thus decreasing the required sample volume even further, and allowing a less traumatic obtrusion.

A 600 μm quartz fiber optic, approximately one meter in length (Math Associates, Port Washington, NY) was stripped of its outer protective coating and inner cladding 1-3/4" from one end. Both ends of the fiber had been carefully cut to ensure no splintering of the blunt fiber which would decrease the numerical aperature of the fiber. The stripped end of the fiber is threaded through the tuberculin syringe and the rubber seal on the plunger. The fiber is inserted into the 19 gauge needle and the cannula attached to the syringe. The opposite end of the fiber is secured by an optical

fiber positioner on an optical bench. The cannula, syringe, and the optical fiber comprises the absorbance probe. The absorbance probe can be made mobile for use in bedside analyses, as previously mentioned, with the use of a fiber optic coupler in each patients' room.

Several probe designs were considered prior to the final design. The first design used a 19 gauge needle that was also cut to form a 90° bevel. This hypodermic needle had a piece of gold optically transparent electrode (OTE) epoxied over the 90° beveled end (Figure 3A). This design would allow aspiration through the OTE and the OTE would permit quantitative reflection. Another design considered was to blacken (Figure 3C) the inner wall of the hypodermic needle. The last design experimentally considered is shown in Figure 3B. The hypodermic needle was lined with a quartz tube in order to produce reflections from an inner reflective surface rather than the stainless steel wall. These design considerations will be discussed in greater detail later.

The optical components used in this work were assembled on an optical table (Figure 4). Radiation (0.025 W at 4579 Å) from the argon ion laser (Spectra-Physics, Model 171) is reflected by a 50 percent beam splitter and focused, using a 35 mm focal length quartz lens, onto the optical fiber. Radiation exiting the terminus of the fiber that is not absorbed is reflected by the aluminum reflector. The nonabsorbed radiation is collected by the fiber optic and transmitted back towards the beam splitter. Fifty percent of this radiation is transmitted through the beam splitter and imaged onto the

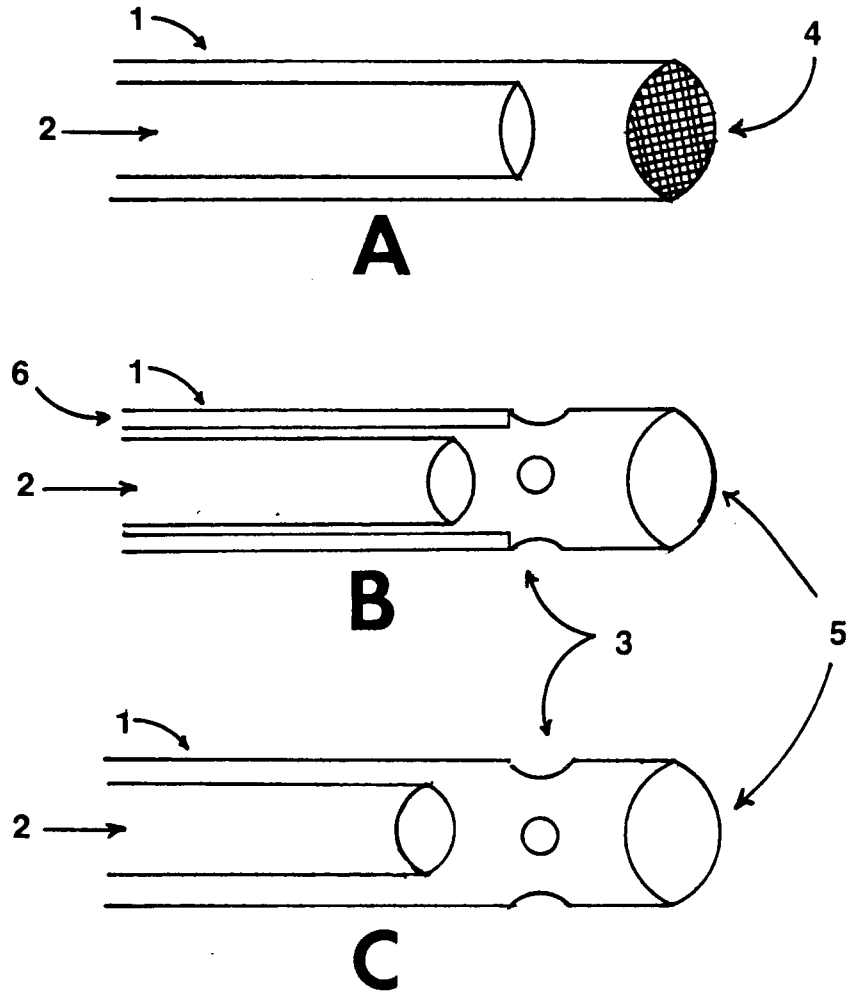

Figure 3. Absorbance probe designs. (A) Optically transparent electrode design, (B) capillary lined design, (C) blackened inner wall design; (1) 19 gauge hypodermic needle, (2) fiber core, (3) aspiration holes, (4) optically transparent electrode, (5) aluminum reflector, (6) quartz capillary.

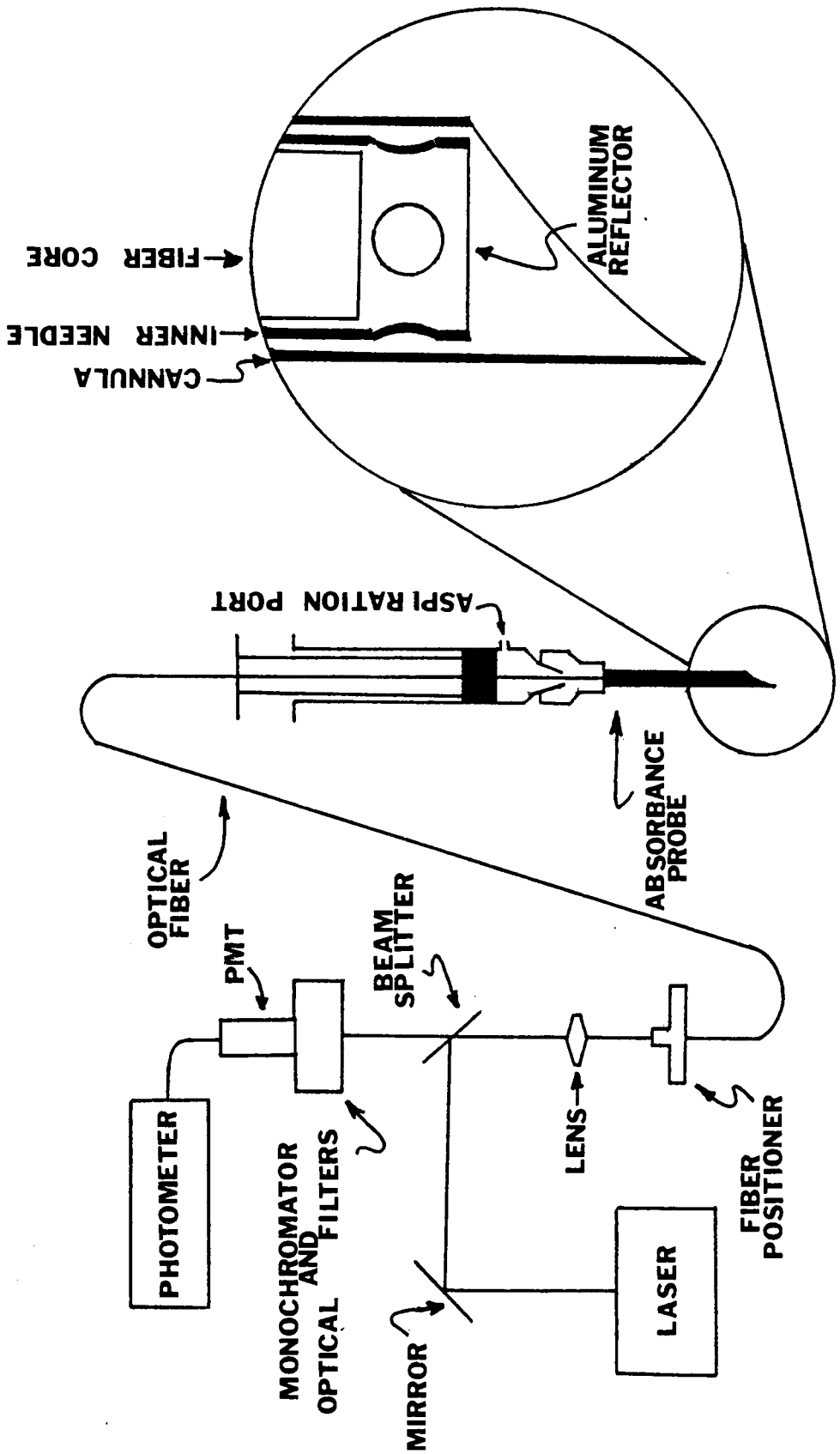

Figure 4. In-vivo absorbance probe apparatus.

entrance slit of a monochromator. An iris positioned between the beam splitter and the entrance slit of the monochromator is used to spatially reject reflected radiation from the surface of the lens and the input end of the optical fiber and to minimize stray room light. Neutral density filters ($10^{5.5}$) were placed between the monochromator and photomultiplier tube (RCA, 1P28-A) to obtain radiation of the proper magnitude for the photomultiplier tube. The voltage for the photomultiplier tube was supplied by a photometer (Pacific Precision Instruments, Model 126). The photocurrent produced by the photomultiplier tube was monitored using the photometer and recorded using a strip chart recorder (Zipp-Konen, Model BD-40).

The argon ion laser, beam splitter, lens, monochromator, neutral density filters, iris, photomultiplier tube, photometer, and recorder comprise the instrumentation. In the bedside analysis scheme, this equipment would be stationary in the hospital with a manifold of optical fibers, each leading to a different patient's room.

In order to determine the optimum pathlength, i.e., the one yielding the greatest sensitivity and lowest detection limits, experiments were conducted with varying pathlengths. Methyl orange, which has a wavelength of maximum absorption nearly coincident with an argon ion laser emission wavelength and is photolytically stable, was used as the analyte for this study. A micrometer attachment (Figure 5) to the experimental apparatus described earlier, made the measurement of the pathlength possible. Three pathlengths were

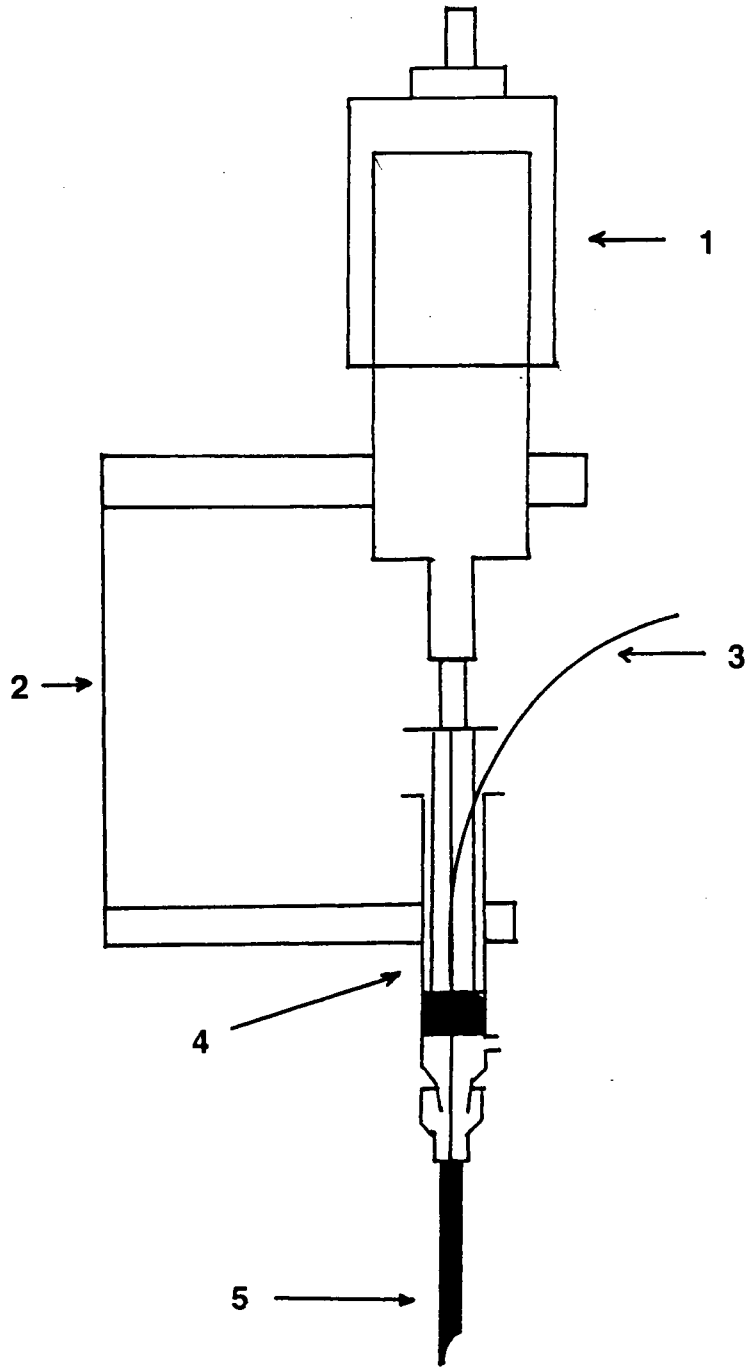

Figure 5. Micrometer attachment. (1) Micrometer, (2) micrometer/syringe holding stand, (3) fiber optic, (4) syringe, (5) absorbance probe.

selected to be studied with six methyl orange standards. The pathlength was set by adjusting the micrometer barrel to the appropriate position. Next, all six standards were introduced into the absorbance probe, one at a time, each followed with a blank. This procedure was repeated four times at each pathlength. Typical chart recordings for a pathlength of 4.3 mm are shown in Figure 6.

The experimental apparatus for the bilirubin in-vitro studies is exactly as described in earlier experiments. The pathlength of the absorbance probe was set at 1.8 mm. Bilirubin standards and human serum samples were obtained from Fisher Chemical Company. Cerebral spinal fluids were obtained from clinical and pathological laboratories. Nonxanthochromic and xanthochromic cerebral spinal fluids were pooled independently to provide common matrices. Reconstitution of all bilirubin standards and preparation of bilirubin containing samples were done under subdued yellow light.

Several different types of experiments were performed using bilirubin as the analyte. In the first experiments bilirubin standards were prepared in an aqueous matrix. Six bilirubin standards were prepared for analysis by dilution of reconstituted bilirubin standards. In the second set of experiments the matrix was cerebral spinal fluid. For these experiments bilirubin analyses were done by a standard addition method in the following manner. First, pooled nonxanthochromic cerebral spinal fluid was spiked to produce a synthetic xanthochromic "sample." Then portions of this "sample"

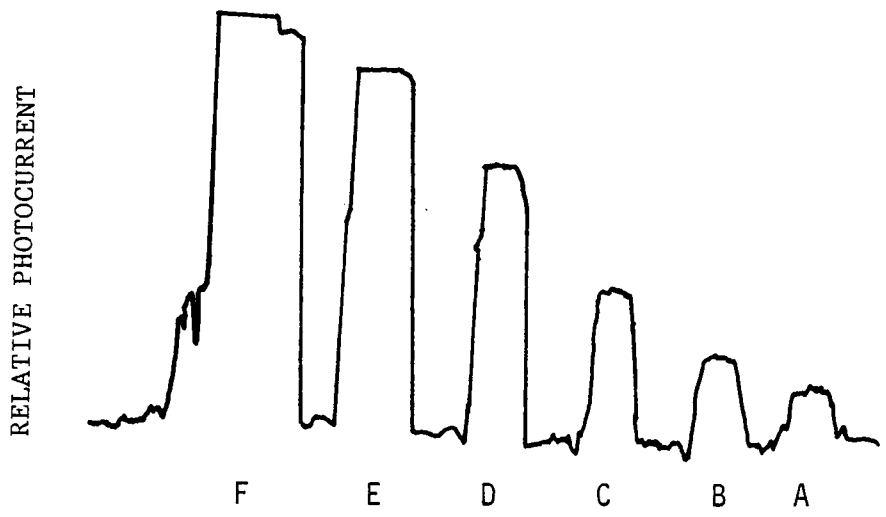

Figure 6. Strip chart recordings of methyl orange standards. (A) 6.40×10^{-6} M; (B) 1.28×10^{-5} M; (C) 3.20×10^{-5} M; (D) 6.40×10^{-5} M; (E) 1.28×10^{-3} M; (F) 2.56×10^{-3} M.

were spiked with reconstituted bilirubin standard for standard addition analyses. Finally, because of the limited availability of cerebral spinal fluid, the last phase of experiments was completed using human serum. In this phase of experimentation reconstituted human serum matrices were spiked with reconstituted bilirubin standards for the preparation of a calibration plot. Four standards were prepared by the author and four double-blind samples were also prepared. Duplicate analyses of all bilirubin samples were performed by The University of Tennessee Memorial Hospital and Research Center using a duPont ACA III.

Typical strip chart recordings for aqueous bilirubin standards, cerebral spinal fluid matrix samples, and human serum matrix standards are shown in Figures 7, 8, and 9, respectively.

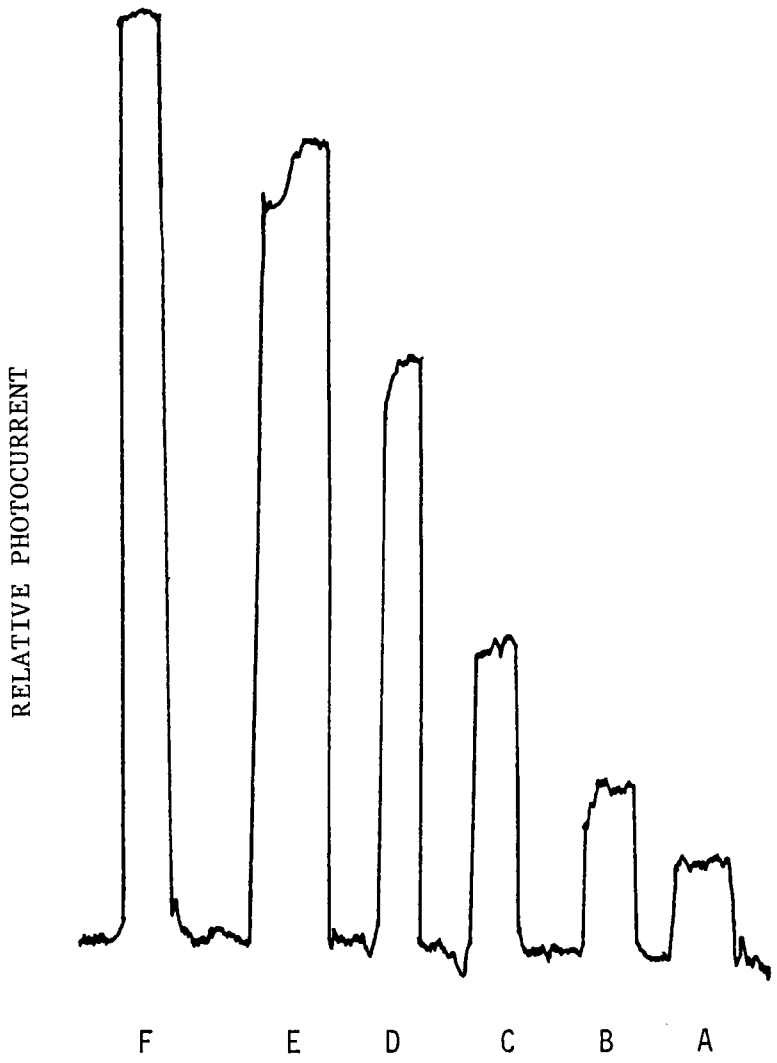

Figure 7. Strip chart recordings for aqueous bilirubin standards. (A) 3.40 x 10^{-6} M, (B) 6.80 x 10^{-6} M, (C) 1.36 x 10^{-5} M, (D) 3.40 x 10^{-5} M, (E) 6.80 x 10^{-5} M, (F) 3.40 x 10^{-4} M.

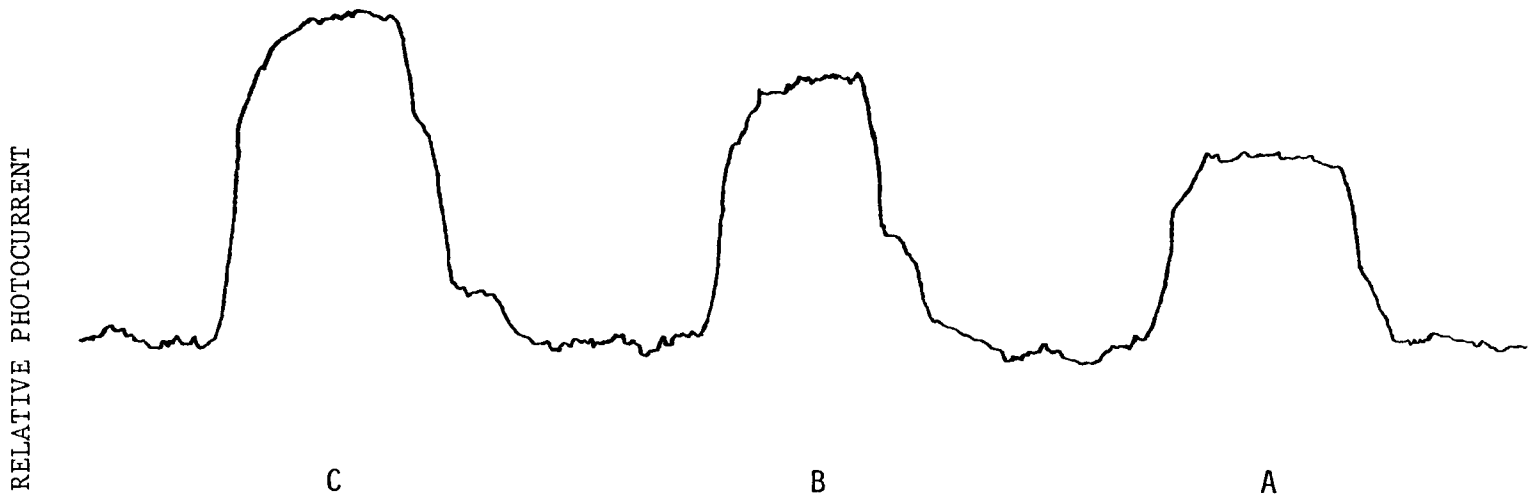

Figure 8. Cerebral spinal fluid matrix strip chart recordings. (A) Synthetically prepared sample, 1.5×10^{-5} M bilirubin, (B) first spiked portion, 1.9×10^{-5} M bilirubin, (C) second spiked portion, 2.2×10^{-5} M bilirubin.

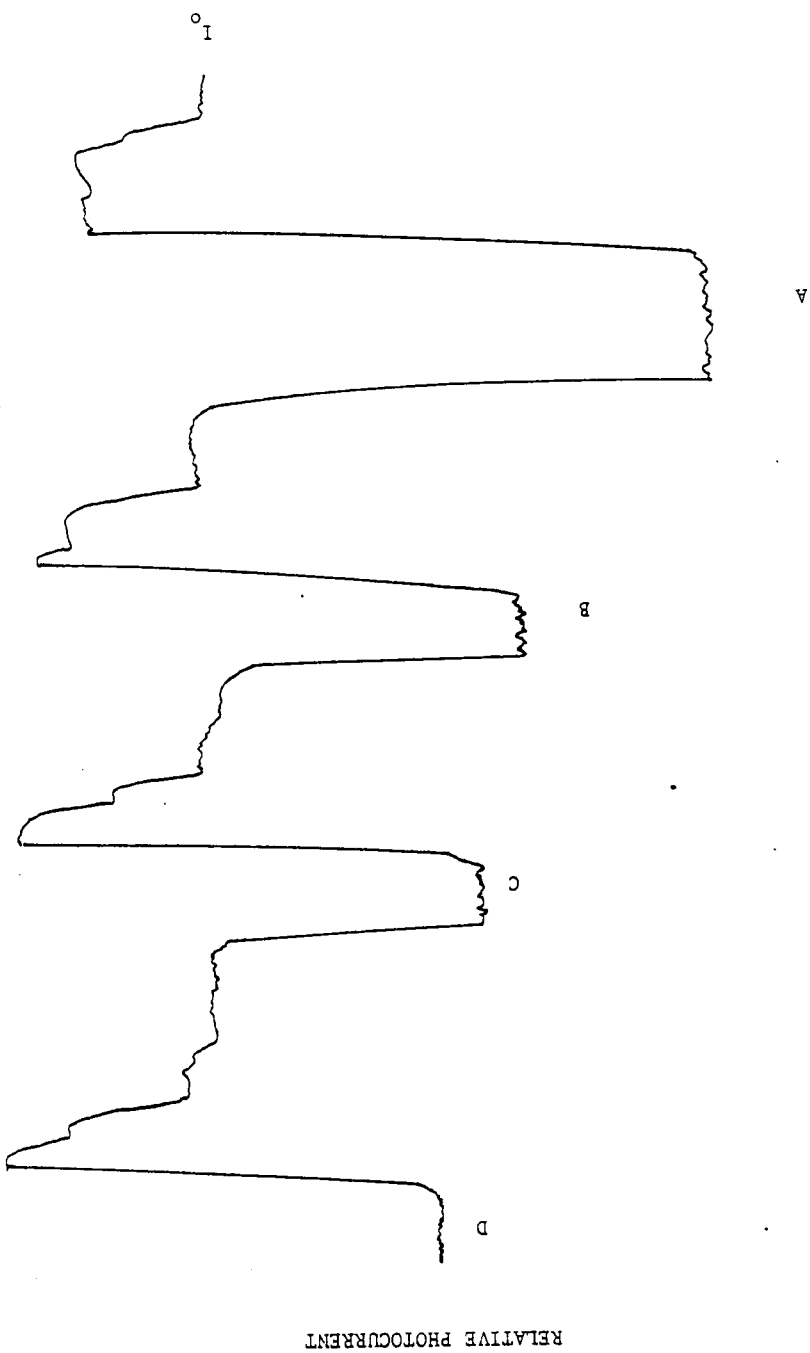

Figure 9. Human serum matrix strip chart recordings. (A) 1.37×10^{-5} M bilirubin, (B) 2.05×10^{-5} M bilirubin, (C) 2.39×10^{-5} M bilirubin; (D) 2.74×10^{-5} M bilirubin.

CHAPTER III

RESULTS AND DISCUSSION

Selection of the best probe was based on my mechanical ability and experimentally encountered problems. First, and quite simply, the probe design utilizing an optically transparent electrode (Figure 4A, page 14) was rejected because of the extreme difficulty in epoxying the OTE without clogging the holes of the OTE.

The basis of the rejection of the other experimental probe designs was more complicated. By increasing the pathlength of the sample cell, the sensitivity will increase proportionally. However, if a constant laser power is maintained and the pathlength is increased a decrease in the reflected radiation is observed. This decrease is attributed to several factors which lead to the rejection of different probe designs. First it was thought that by blackening the inner wall of the hypodermic needle photons that collide with the inner wall would be absorbed, thus decreasing the possibility of multiple pathlengths which would produce a nonlinear relationship between absorbance and concentration. One problem with this design is the difficulty encountered in blackening the inner wall of the needle. Because any radiation not normal to the fiber terminus was absorbed by the wall of the needle, a severe decrease in the reflected radiation was seen. In order to compensate for this decrease in reflected radiation the laser power was increased. However, when the laser power was increased the stray radiation also increased, since stray

radiation is a fraction of incident power (SI_0). Stray radiation may be defined in several different ways, but for our purposes it represents radiation that strikes the detector that has not passed through the sample cell. Also, when large laser powers are used thermal problems are encountered in the absorbance probe, such as boiling the sample. Since the magnitude of the stray radiation problem seemed to far exceeded the multiple pathlength problem my attention turned to making the inner wall of the hypodermic needle highly reflective in hopes that the envisioned multiple pathlength problem would experimentally prove to have little or no effect on the linearity of Beer's Law plots.

A probe design using a quartz capillary was to function similar to enhanced fiber Raman spectroscopy (19). In enhanced fiber Raman spectroscopy a capillary optical fiber is filled with a sample solution. Provided the refractive index of the liquid core is greater than the refractive index of the fiber, radiation traveling in the liquid core at an angle less than the critical angle will be trapped in the core. This relationship is provided by Snell's Law, equation 1,

$$n_1 \sin \theta = n_c \sin \theta' \qquad (1)$$

where n_1 and n_c are refractive indices of the liquid core and capillary respectively, θ and θ' are the angles of the incidence and refraction, respectively. For the critical angle, θ_c, when $\theta' = 0$,

$$\sin \theta_c = \frac{n_c}{n_1} . \qquad (2)$$

Fused silica quartz has a refractive index of 1.463 at 4880 A and most aqueous solutions, such as body fluids, have refractive indices less than 1.463 at 4880 A, which means that refraction will occur into the capillary. Obviously this method would not work, so the capillary was modified by depositing silver using Tollens reagents on the inside of the capillary to provide specular reflection from the inner capillary wall, before refraction could occur. This did not provide a thoroughly even coat of silver to effect the reflective surface desired. Next an attempt was made to cathodically sputter aluminum from a thin tungsten wire threaded through the capillary which was suspended inside a vacuum chamber. Because of the high vapor pressure of aluminum, it could not be vaporized efficiently without clogging the capillary. Therefore it was not possible to utilize this design.

It should be noted at this time that the current probe is far from optimum, in terms of greatest reflectivity of laser radiation by the inner hypodermic needle wall. However, due to the limited availability of mechanical expertise, it was necessary to use the current design.

In a two fiber probe design (16), laser excitation radiation could be transmitted through the sample through one fiber and non-absorbed reflected radiation would be transmitted to the detector via the second fiber. This design eliminates the need for the beam splitter but poses additional problems. For instance, since the fiber collecting the nonabsorbed reflected radiation cannot be

coincident with the excitation radiation fiber, the quantity of reflected radiation will be very small. In order to compensate for this small signal, the laser power will have to be increased. This will cause additional problems like the aforementioned thermal effects. Also, because two fibers are used the sum of the diameters of the fibers must be smaller than the inner diameter of the inner hypodermic needle or the diameters of the hypodermic needles must be increased to accommodate the two fibers. Theoretically, the diameter of the fiber should be limited to the obtainable beam waist of the laser. In light of these foreseeable problems, this design was not experimentally considered.

While determining the optimum pathlength, the problem of stray radiation was discovered. For the calculations of absorbances in these experiments the intensities of the incident (I_0) and attenuated (I) radiations were measured. I_0 was determined by measuring the reflected radiation with the blank in the absorbance probe. I was determined when each standard was introduced into the absorbance probe. Absorbances were calculated using Beer's Law, equation 3.

$$A = \varepsilon\, b\, c = \log \frac{I_0}{I} \qquad (3)$$

Beer's Law plots of the data are represented in Figure 10. Error bars represent the highest and lowest values obtained. Negative deviation seen at high concentrations can be due to several things, including stray radiation. The effect on Beer's Law is seen in equation 4.

$$A = \log \frac{I_0 + SI_0}{I + SI_0} \qquad (4)$$

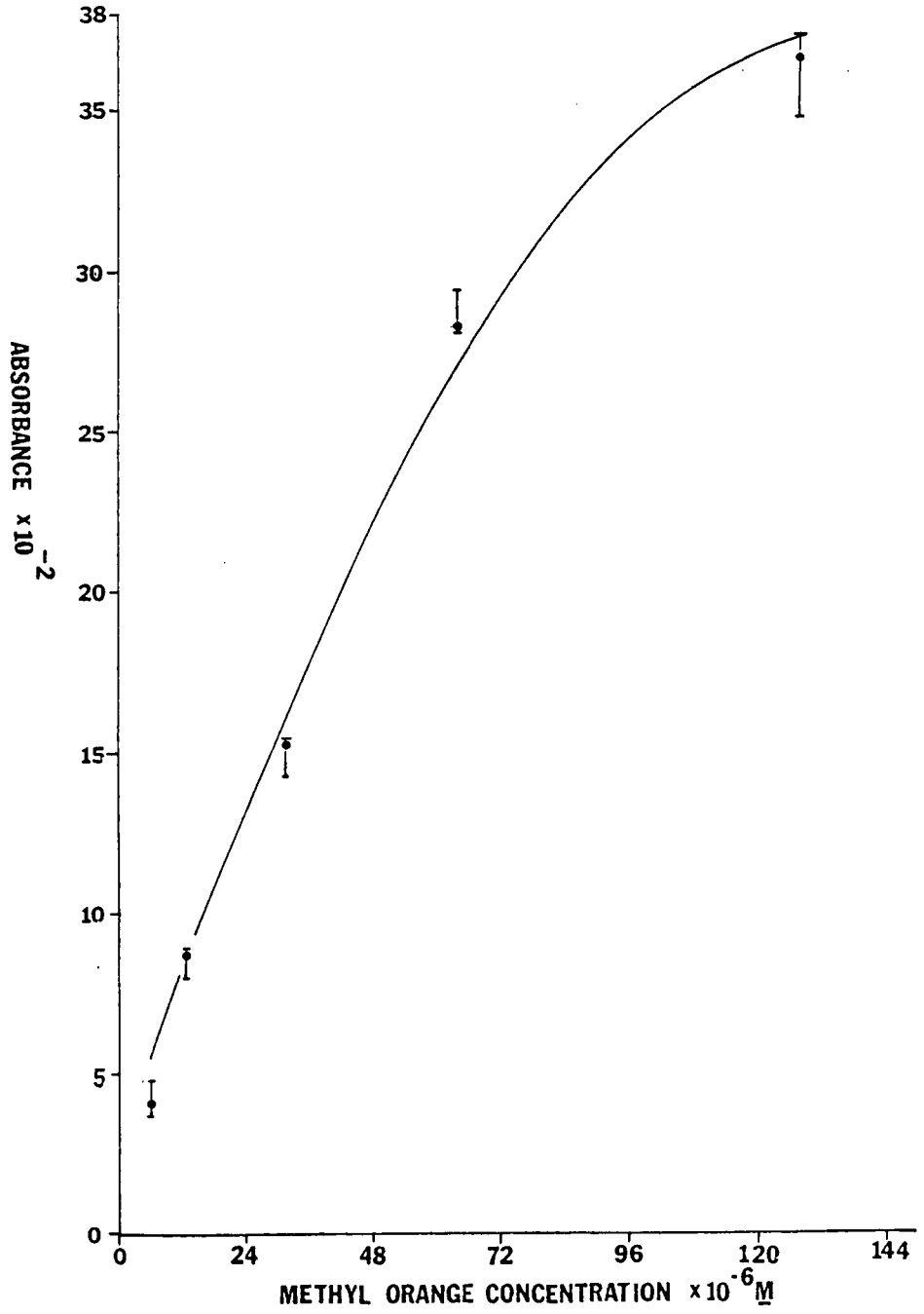

Figure 10. Beer's Law plot for methyl orange standards (uncorrected).

Therefore absorbance values calculated when stray radiation is not compensated for are incorrect. One way to compensate for stray radiation is by subtracting the intensity of that stray radiation. That intensity may be determined by measuring the intensity of radiation that strikes the detector when a strongly absorbing solution fills the absorbance cell so that all of the light eminating from the fiber terminus is absorbed. Under these circumstances the radiation that strikes the detector must be reflected radiation from the beam splitter, lens, front face of the optical fiber/air interface and fiber terminus/solution interface. Any radiation that propagates past the fiber terminus/solution interface is not considered to be stray light. By subtracting the correction fraction of I_0 for stray radiation in the Beer's Law expression in equation 4, an accurate value for the absorbance may be calculated. Now, after correcting the data in Figure 10 for stray radiation, it has been replotted in the top curve of Figure 11.

As seen in Figure 11, when the concentration of serial standard increases, the confidence interval increases. This is because as the concentration increases, I approaches SI_0. When this happens, the precision of the SI_0 measurement limits the precision of the calculated absorbance values. This is because of the large error encountered when subtracting two relatively close numbers. Also, as the pathlength increases, the magnitude of I decreases and approaches SI_0, due to the absorption of radiation by the inner wall of the hypodermic needle. Once again the error in calculating the absorbances

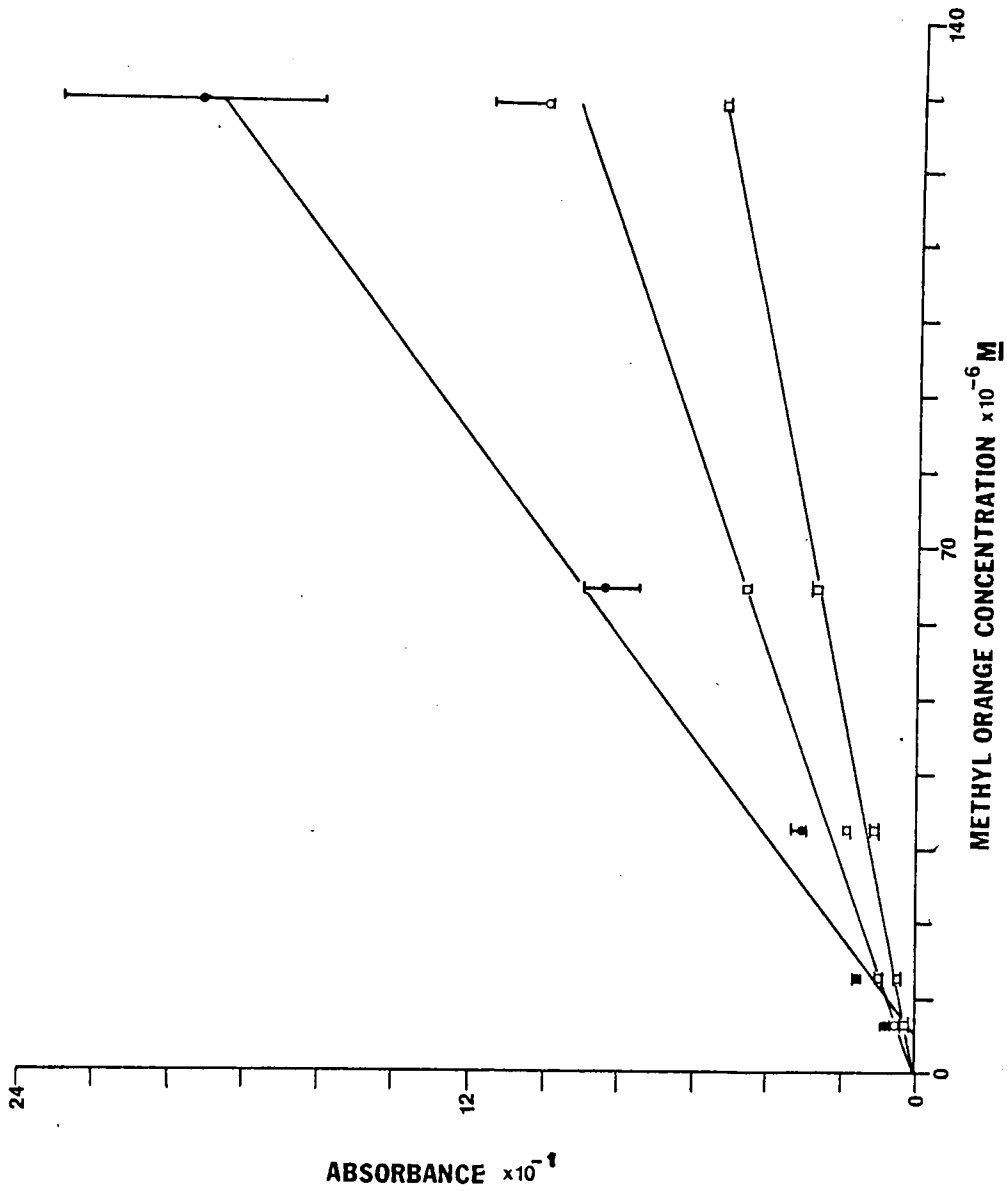

Figure 11. Beer's Law plot for methyl orange standards at varying pathlengths. ● = 4.3 mm; ○ = 1.8 mm; □ = 0.5 mm.

increases for the same reason just stated. These trends are seen in Figure 11 too.

For the determination of limits of detection for each pathlength the origin area of the figure has been expanded (Figure 12). Perpendiculars representing the limit of detection for each pathlength at a signal-to-noise ratio of 2 (S/N = 2), have been drawn in Figure 12. For the pathlength of 4.3 mm, a corrected linear regression line using the low concentration methyl orange standards was drawn. This is justified due to the large error bars seen at high concentrations of methyl orange. Table I shows I_0, noise, limits of detection, and correlation coefficients for each pathlength.

From the data presented in Table I, the optimum pathlength was chosen to be 1.8 mm. This choice was based on the fact that the lowest limit of detection and moderate sensitivity was seen with the 1.8 mm pathlength.

In all in-vitro experiments, except for the human serum experiments, I_0 was determined by measuring the reflected radiation when water was drawn into the absorbance probe. For the human serum experiments I_0 was determined by measuring the reflected radiation when the serum matrix was drawn into the absorbance probe. I was determined by measuring the attenuated reflected radiation when a standard or sample was drawn into the absorbance probe. SI_0 was determined by measuring the reflected radiation when virtually all of the emitted radiation was absorbed by a concentrated bilirubin

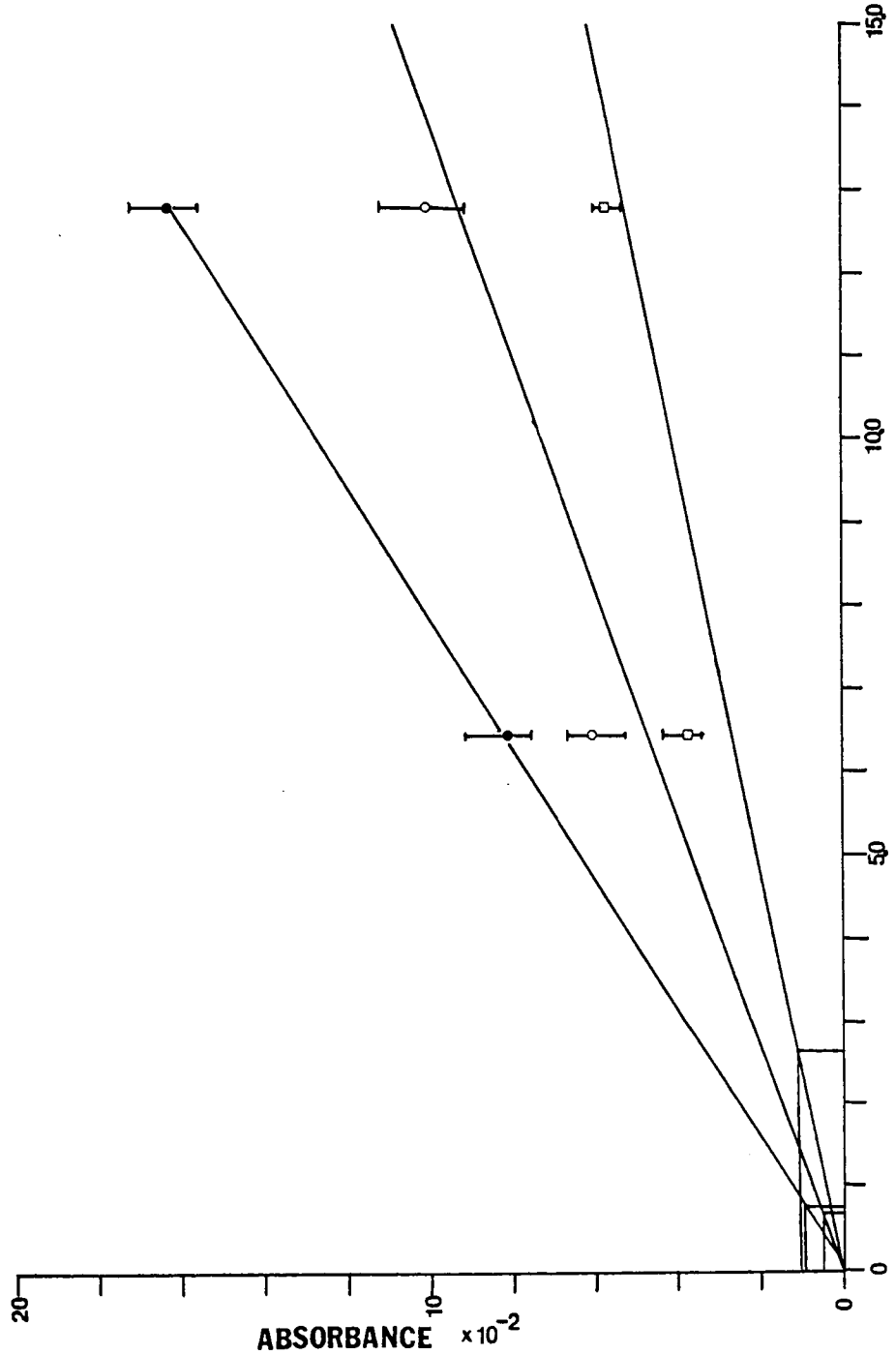

Figure 12. Exploded origin area of methyl orange Beer's Law plots.

TABLE I

METHYL ORANGE EXPERIMENTAL RESULTS

Pathlength, mm	Noise, nA	I_o, nA	LOD, Absorbance Units	Correlation Coefficient
4.3	0.5	77	0.009	0.993
1.8	1.0	111	0.005	0.998
0.5	1.5	150	0.011	0.998

standard solution. Calculation of the absorbance values were performed in the usual manner.

Beer's Law plots for aqueous bilirubin standards are shown in Figure 13. Calculated linear regression constant of 0.999 was obtained for this data. An enlarged plot of the origin area of Figure 13 is shown in Figure 14 with perpendiculars representing the limit of detection at a signal-to-noise ratio equal to two. Error bars are also graphically depicted in Figures 13 and 14.

A typical standard addition plot for a pooled xanthochromic cerebral spinal fluid sample is shown in Figure 15. Table II shows the data collected for two nonxanthochromic cerebral spinal fluid (NXCSF) samples and two xanthochromic cerebral spinal fluid samples (XCSF).

Duplicate analyses of each sample were performed using a duPont ACA III. The standard neonatal bilirubin (NBili) method is a direct spectrophotometric method that subtracts the absorbance at 540 nm (λ_{min} for bilirubin) from the absorbance at 450 nm (λ_{max} for bilirubin). This bichromatic method corrects the interfering species oxyhemoglobin and hemoglobin, which have approximately the same molar absorptivity at 450 nm and 540 nm. Bilirubin concentration values obtained using the absorbance probe are also tabulated with actual values for synthetically prepared samples.

Results in Table II indicate that the experimental bilirubin concentrations obtained using the probe for two nonxanthochromic cerebral spinal fluid (NXCSF) samples yielded slightly higher values

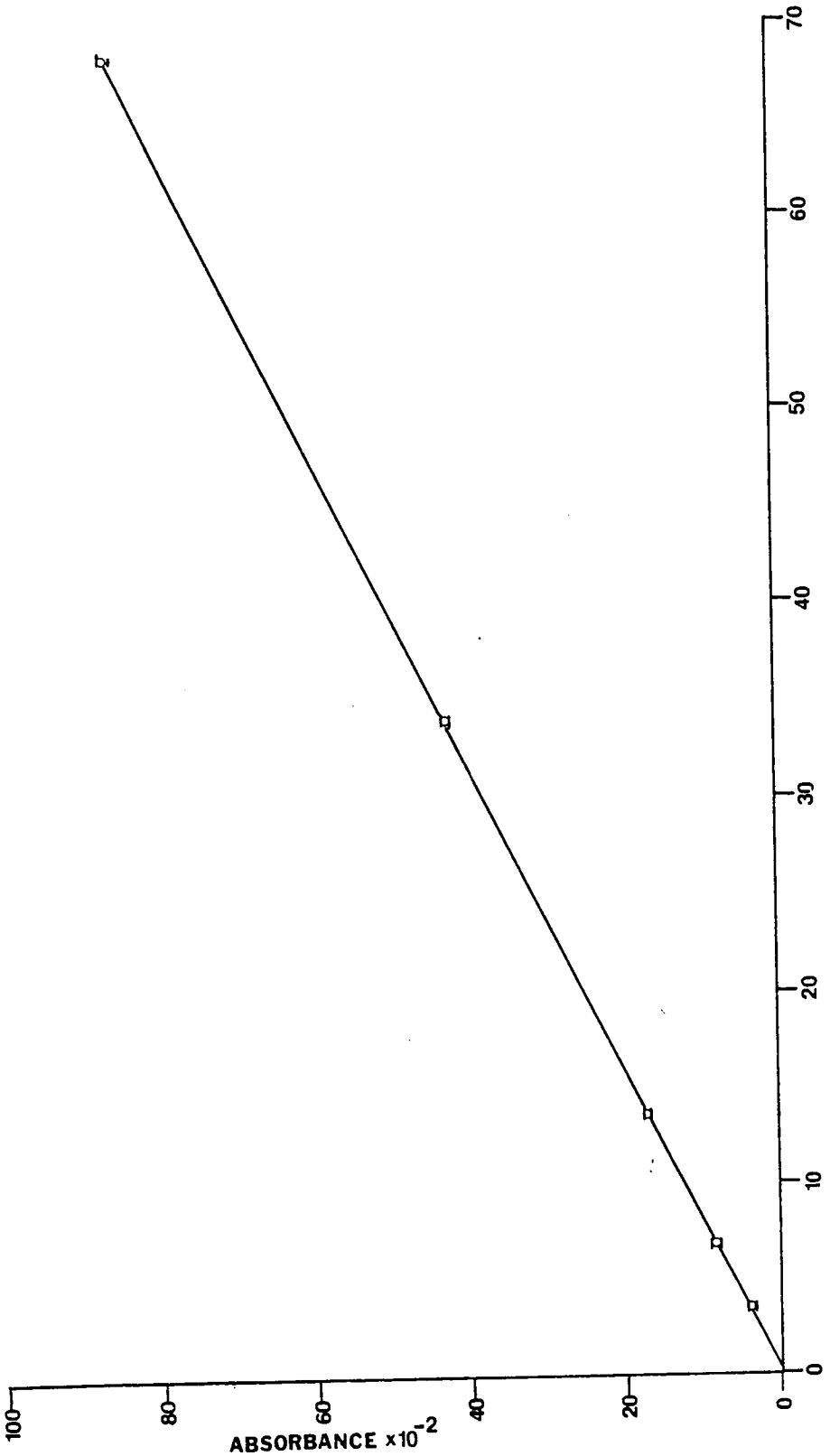

Figure 13. Beer's Law plot of aqueous bilirubin standards.

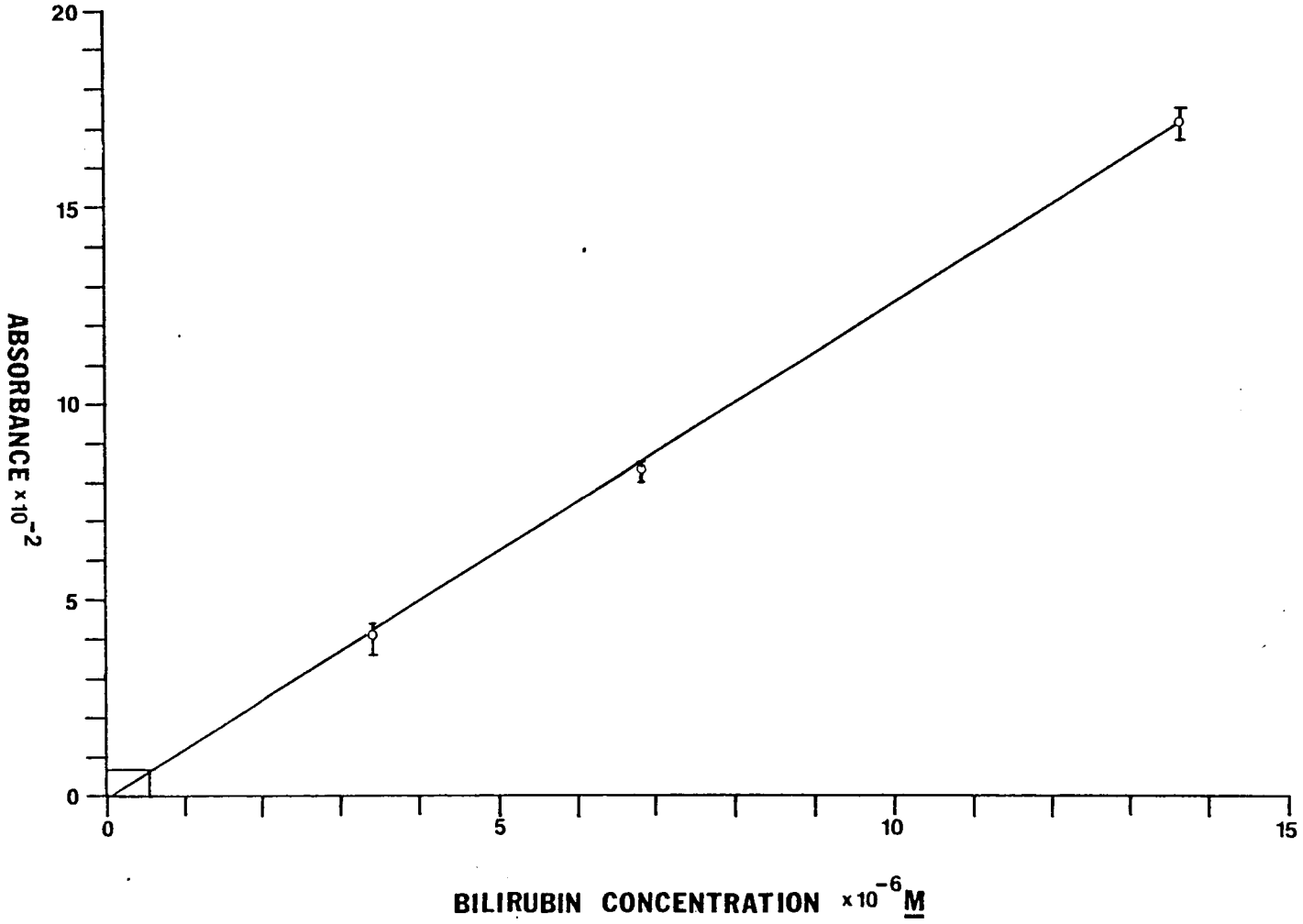

Figure 14. Exploded origin area of Figure 13 for determination of limits of detection for aqueous bilirubin standards.

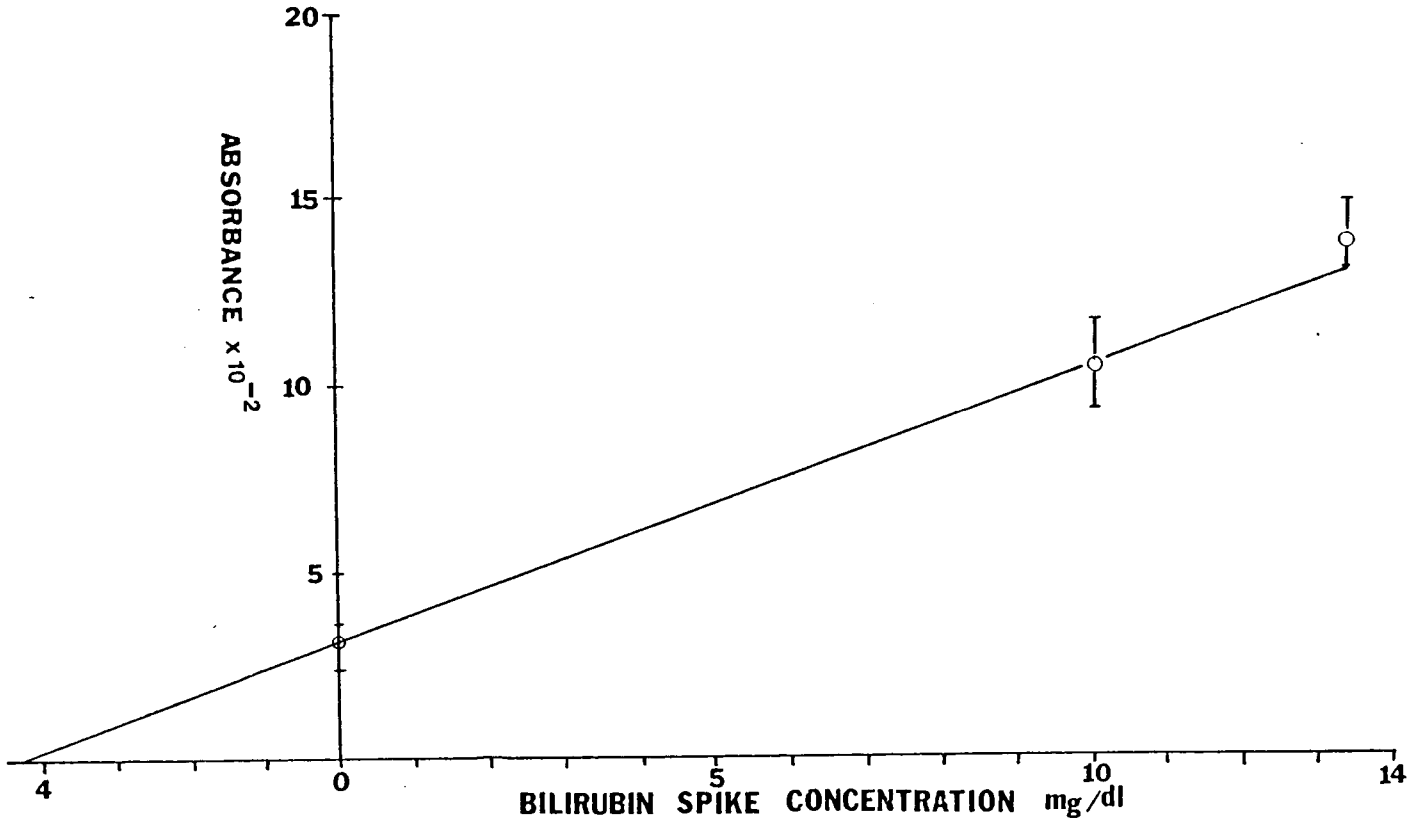

Figure 15. Standard addition plot for a pooled xanthochromic cerebral spinal fluid sample.

TABLE II

CEREBRAL SPINAL FLUID EXPERIMENTAL RESULTS

Sample	Probe, mg/dl	NBili, mg/dl	Actual, mg/dl
NXCSF	1.0	0.99	0.88
NXCSF	0.8	1.13	0.80
XCSF	2.45	1.0	
XCSF	4.25	0.4	

than the true bilirubin concentration values. The true concentration values represent the subsequent concentration of bilirubin due only to the addition of reconstituted bilirubin standard to a portion of the pooled NXCSF. The difference observed in these two values can be due to the difficulty in obtaining cerebral spinal fluid that is completely nonxanthochromic, that is, it must contain no trace of bilirubin or any interfering species which would lead to erroneously large absorbances. For the two xanthochromic cerebral spinal fluid (XCSF) samples the bilirubin concentration obtained using the probe was much greater than the duPont ACA III NBili method. Since the probe is a monochromatic method, absorbance due to the interfering compounds in the XCSF samples cannot be corrected for as in the NBili bichromatic method. Therefore, the standard addition plot will lead to an erroneously large concentration for bilirubin. However, recognizing this fact, the absorbance probe could be adapted for bichromatic analyses as stated earlier and outlined in the Appendix.

A calibration plot for the human serum matrix experiment is shown in Figure 16 with perpendiculars representing four double-blind samples. A calculated linear regression constant of 0.986 was obtained for this data. Bilirubin concentration values for the four samples were obtained by solving the equation for a straight line using linear regression data obtained for four bilirubin standards.

For the human serum experiments I_0 was determined while aspirating the normal human serum matrix, which contains a normal level of bilirubin, into the absorbance probe. Therefore calculated absorbance

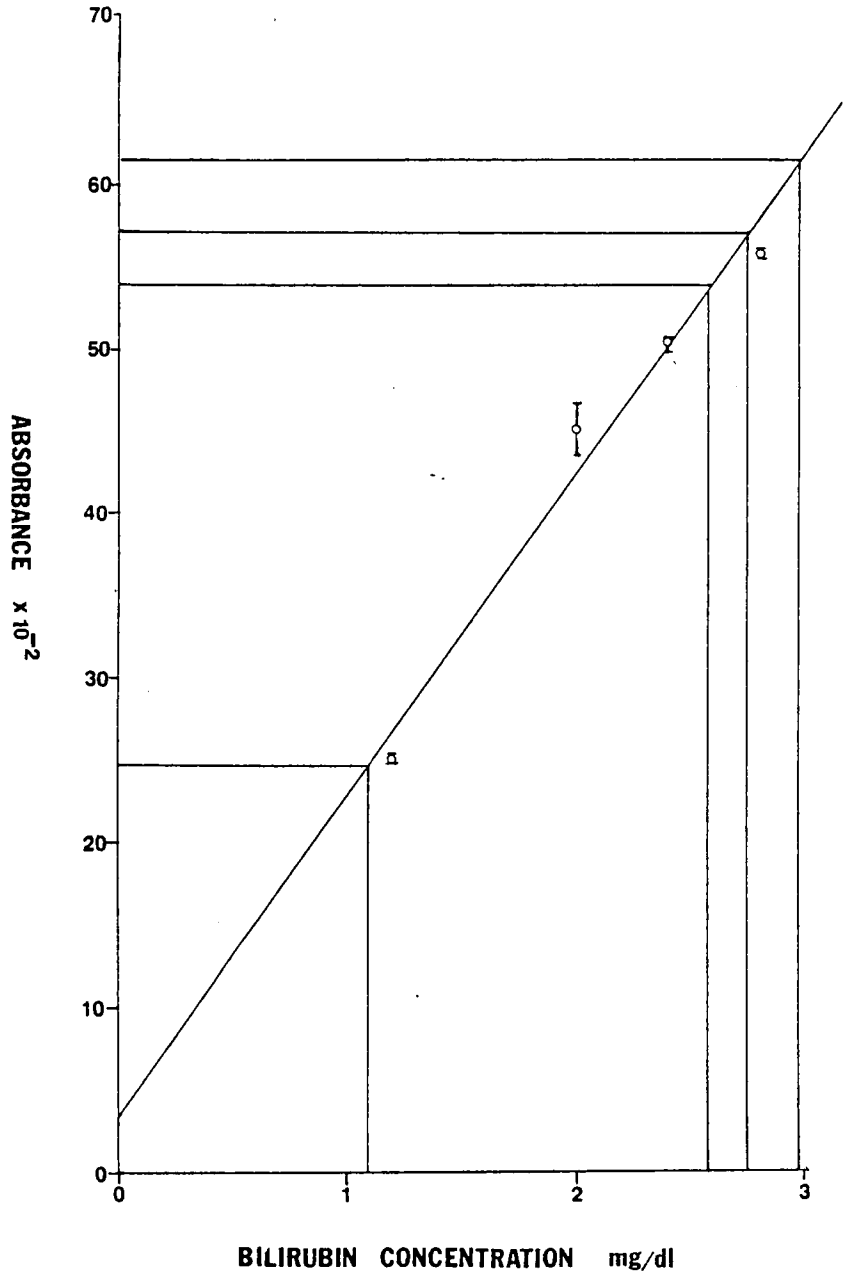

Figure 16. Calibration plot for human serum experimentation.

values correspond only to the amount of bilirubin added to the normal serum matrix. NBili values were obtained on all double-blind samples.

In order to obtain a comparable value from the duPont ACA III, the NBili value for the normal human serum matrix was subtracted from the NBili value for each double-blind sample. These data are listed in Table III.

The NBili method, as stated by duPont, should never be used with serum from neonates that are greater than 21 days of age due to the presence of carotenes and other pigments in the serum which are not corrected for using this bichromatic method. The human sera purchased for this experiment were prepared from adult sera which do contain carotenes and other pigments. Therefore, the bilirubin concentration value obtained using the duPont ACA III will be incorrect. This could account for the discrepancy between the NBili-SERUM values and the actual values.

TABLE III

HUMAN SERUM EXPERIMENTS

Probe, mg/dl	Actual, mg/dl	NBili-Serum, mg/dl
1.10	1.07	0.0
2.58	2.60	2.15
2.97	3.01	2.85
2.74	2.77	2.55

CHAPTER IV

CONCLUSIONS

The in-vivo absorbance probe described herein has many unique advantages over current clinical methodologies as outlined earlier. Reemphasizing the major characteristics:

1. extremely small sample volume requirements,
2. no removal of sample from host environment,
3. no disruption of equilibrium,
4. possible reduction in analysis time,
5. safer obtrusion into hostile environments,
6. continuous monitoring of a dynamic system,
7. no exposure to ambient light, and
8. relatively low equipment cost.

In-vitro experimentation using the absorbance probe has revealed several facts. First, remote measurements using the absorbance probe for the determination of true absorbance values are possible. Next, the extension of this concept with a body chemical, namely bilirubin, in an aqueous matrix is also possible. Further extension of this concept in a true body matrix is possible but will require adaptation of the existing prototype. This adaptation was referred to earlier and outlined in the Appendix as the bichromatic analysis system. Realistic problems with interfering species in body fluids can be and are dealt with using current in-vitro diagnostic laboratory instrumentation incorporating a bichromatic method.

In light of the conclusive experimentation performed in this thesis, in-vivo absorbance measurements should be possible using the absorbance probe instrumentation.

LIST OF REFERENCES

LIST OF REFERENCES

1. Teitz, N. Fundamentals of Clinical Chemistry. W. B. Saunders, Philadelphia, 1976, pp. 187-188.

2. Hercules, D. M., Hieftje, Snyder, L. R., and Evenson, M. A. Contemporary Topics in Analytical and Clinical Chemistry. Plenum Press, New York, 1982, Vol. 3, p. 27.

3. Baird, J. L. British Patent Specification No. 20,969/27. 1927.

4. Lamm, H. Z. InstrumKde, 1930, 50, 579.

5. Berci, G. and Davids, J. Brit. M. J., 1962, 1, 1610.

6. Coleman, J. A., Bereskin, S. and Shackney, C. N. Engl. J. Med. 1965, 273, 26, 1525.

7. Hugenholtz, P. G., Gamble, W. J., Monroe, R. G., and Polanyi, M. Circulation, March 1965, 31, 344.

8. Taylor, J. B., Lown, B. and Polanyi, M. JAMA, 1972, 221, 7, 667.

9. McCarthy, B., Hood, W. B. Jr., and Lown, B. J. Appl. Physiol. 1967, 23, 5, 641.

10. Singh, R., Runieri, A. J. Jr., Vest, H. R. Jr., Bowers, D. L. and Dammann, J. F. Jr. Am. J. Cardi., 1970, 25, 579.

11. Renault, G., Raynal, E., Sinet, M., Berthier, J. P., Goddard, B. and Cornillault, J. Opt. Laser Technol., June 1982, 142.

12. Suidan, J. S. and Young, B. K. Clin. Chem., 1982, 29, 8, 1566.

13. Klainer, S., Hirschfeld, T., Brown, H., Milanovich, E., Perry, D. and Johnson, D. A monitor for detecting nuclear waste leakage in a subsurface repository, Lawrence Berkley Laboratory, University of California, Berkley, LBL-11981, UC-70, 1980.

14. Borman, S. A. Anal. Chem., 1981, 53, 1616A.

15. Seitz, W. R. Anal. Chem., 1984, 56, 16A.

16. Oriel Corporation, Instrumentation for Spectroscopy and Detection, 250 Long Beach Blvd., Stratford, CT 06497-0872, 1983, 96.

17. Demtröder, W. Laser Spectroscopy. Springer-Verlag, Berlin, New York, 1981. Springer Series in Chemical Physics, 5, p. 273.

18. Personal communication with Dr. P. Painter, The University of Tennessee Memorial Hospital and Research Center, Alcoa Highway, Knoxville, TN, January 1984.

19. Walrafen, G. E. and Stone, J. Appl. Spectrosc., 1972, 26, 6, 585.

APPENDIX

APPENDIX

A two-laser system, positioned so that laser beam 1 is coincident with laser beam 2, with the use of a dichroic filter positioned between laser 1 and laser 2, is needed for bichromatic analyses. The dichroic filter must be selected so that it is optically transparent to laser 1 and reflective with respect to laser 2. The intensities of the reflected nonabsorbed radiation at the two wavelengths may be measured independently and subsequent absorbance calculations performed. See Figure A-1.

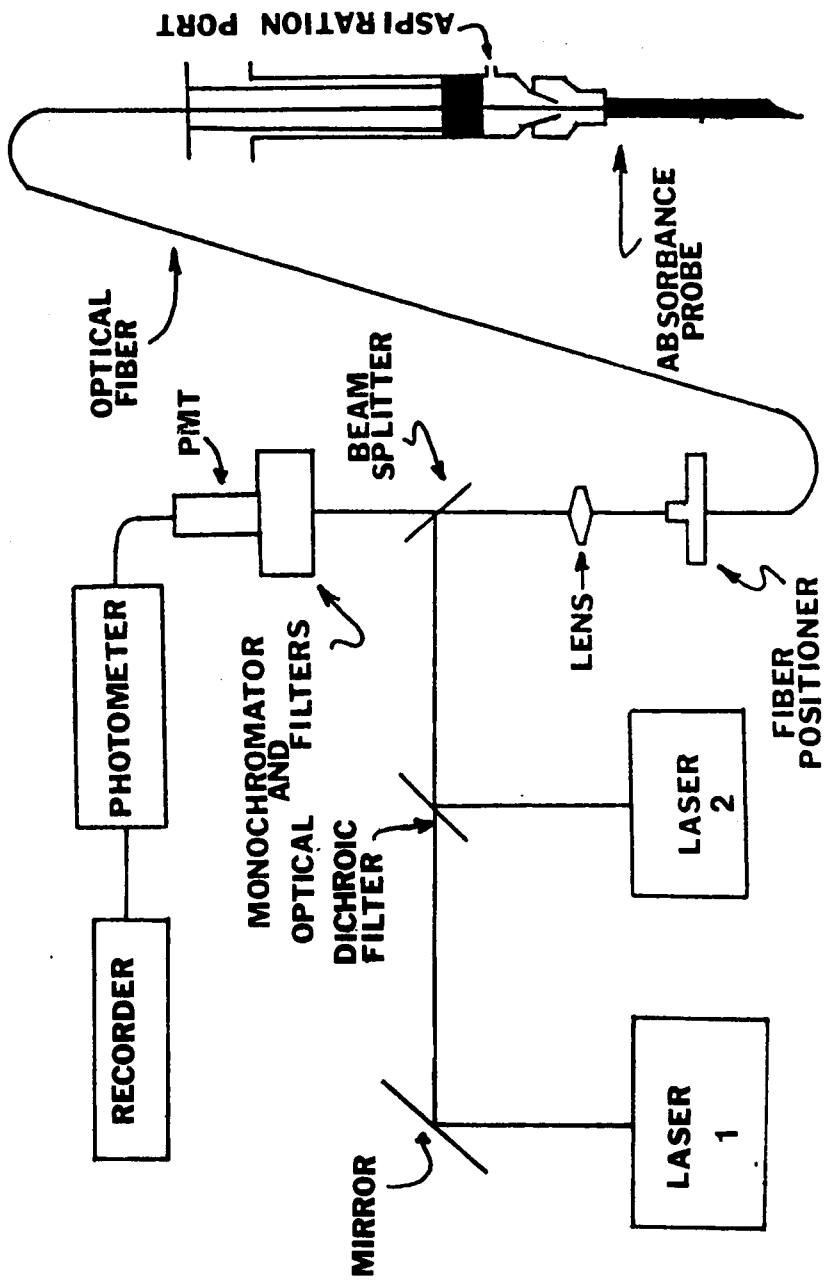

Figure A-1. Instrumental design for bichromatic in-vivo absorbance analyses.

VITA

Jerry Todd Coleman was born in Humboldt, Tennessee on December 29, 1957. He attended elementary school in Memphis, Tennessee and Shelby County, Tennessee. He graduated from Germantown High School, Germantown, Tennessee in 1975. He graduated from Memphis State University in May 1980 with a Bachelor's degree in Chemistry. In the fall of 1981 he began graduate work at The University of Tennessee, Knoxville, after accepting a graduate teaching assistantship. Graduation followed in the spring of 1984 with a Master of Science degree with a major in Chemistry.

The author is a member of Phi Lambda Upsilon (Honorary Chemistry Fraternity), The American Chemical Society, The Society for Applied Spectroscopy, and The Association of Chemistry Graduate Students.

He will be employed at E. I. duPont de Nemours and Company, Atomic Energy Division, Savannah River Plant, Aiken, South Carolina beginning May 1, 1984 and also will have the good fortune of marrying Susan Elaine Acuff of Knoxville, Tennessee on June 23, 1984.